

# Inhibition of Glycogen Synthase Kinase-3 Ameliorates $\beta$ -Amyloid Pathology and Restores Lysosomal Acidification and Mammalian Target of Rapamycin Activity in the Alzheimer Disease Mouse Model

## IN VIVO AND IN VITRO STUDIES\*

Received for publication, August 9, 2012, and in revised form, November 12, 2012. Published, JBC Papers in Press, November 15, 2012, DOI 10.1074/jbc.M112.409250

Limor Avrahami<sup>†1</sup>, Dorit Farfara<sup>§1</sup>, Maya Shaham-Kol<sup>‡</sup>, Robert Vassar<sup>¶</sup>, Dan Frenkel<sup>§2</sup>, and Hagit Eldar-Finkelman<sup>†3</sup>

From the <sup>†</sup>Departments of Human Molecular Genetics and Biochemistry, Sackler School of Medicine and the <sup>§</sup>Department of Neurobiology, George S. Wise Faculty of Life Sciences, Tel Aviv University Tel Aviv 69978, Israel and the <sup>¶</sup>Department of Cell and Molecular Biology, Northwestern University Feinberg School of Medicine, Chicago, Illinois 60611

**Background:** The mechanisms behind the contribution of GSK-3 to Alzheimer disease pathogenesis remain elusive.

**Results:** A GSK-3 inhibitor reduced A $\beta$  pathology and ameliorated cognitive decline in an Alzheimer disease mouse model. GSK-3 impairs lysosomal acidification and impacts mTOR activity.

**Conclusion:** Inhibition of GSK-3 reverses Alzheimer disease pathogenesis via restoration of lysosomal acidification and reactivation of mTOR.

**Significance:** We identified novel mechanisms linking GSK-3 with A $\beta$  pathology.

Accumulation of  $\beta$ -amyloid (A $\beta$ ) deposits is a primary pathological feature of Alzheimer disease that is correlated with neurotoxicity and cognitive decline. The role of glycogen synthase kinase-3 (GSK-3) in Alzheimer disease pathogenesis has been debated. To study the role of GSK-3 in A $\beta$  pathology, we used 5XFAD mice co-expressing mutated amyloid precursor protein and presenilin-1 that develop massive cerebral A $\beta$  loads. Both GSK-3 isozymes ( $\alpha/\beta$ ) were hyperactive in this model. Nasal treatment of 5XFAD mice with a novel substrate competitive GSK-3 inhibitor, L803-mts, reduced A $\beta$  deposits and ameliorated cognitive deficits. Analyses of 5XFAD hemi-brain samples indicated that L803-mts restored the activity of mammalian target of rapamycin (mTOR) and inhibited autophagy. Lysosomal acidification was impaired in the 5XFAD brains as indicated by reduced cathepsin D activity and decreased *N*-glycosylation of the vacuolar ATPase subunit V0a1, a modification required for lysosomal acidification. Treatment with L803-mts restored lysosomal acidification in 5XFAD brains. Studies in SH-SY5Y cells confirmed that GSK-3 $\alpha$  and GSK-3 $\beta$  impair lysosomal acidification and that treatment with L803-mts enhanced the acidic lysosomal pool as demonstrated in LysoTracker Red-stained cells. Furthermore, L803-mts restored impaired lysosomal acidification caused by dysfunctional presenilin-1. We provide evidence that mTOR is a target activated by GSK-3 but inhibited by impaired lysosomal acidification and elevation in amyloid pre-

cursor protein/A $\beta$  loads. Taken together, our data indicate that GSK-3 is a player in A $\beta$  pathology. Inhibition of GSK-3 restores lysosomal acidification that in turn enables clearance of A $\beta$  burdens and reactivation of mTOR. These changes facilitate amelioration in cognitive function.

Increased production of amyloid  $\beta$  (A $\beta$ )<sup>4</sup> peptides and accumulation of A $\beta$  plaques are key hallmarks of Alzheimer disease (AD) pathogenesis. A $\beta$  peptides are considered major mediators of the development of brain lesions characteristic of AD (1–3). The 40- or 42-residue peptides (A $\beta$ <sub>40</sub> and A $\beta$ <sub>42</sub>) are generated by sequential proteolysis of the amyloid precursor protein (APP) catalyzed by  $\beta$ -secretase,  $\beta$ -site APP cleaving enzyme 1, and presenilin-dependent  $\gamma$ -secretase (1–3). Progressive accumulation of A $\beta$  peptides enhances fibrillogenic assembly and formation of A $\beta$  load burdens exerting toxic and disruptive effects on neurons, synaptic plasticity, and cognitive functions (1, 4, 5). Reducing the accumulation of A $\beta$  deposition is thus believed to be a useful therapeutic strategy (6), and extensive research has aimed at understanding the processes governing APP proteolysis, A $\beta$  stability, and A $\beta$  clearance.

Glycogen synthase kinase-3 (GSK-3) is an evolutionary conserved serine/threonine kinase expressed as two isozymes: GSK-3 $\alpha$  and GSK-3 $\beta$  (7). Hyperactive GSK-3 has been implicated in the etiology of neurodegenerative diseases including Parkinson disease, amyotrophic lateral sclerosis, AD, and brain aging (8–12). Aberrant phosphorylation of AD-related compo-

\* This work was supported by Israel Science Foundation Grant 341/10 and Seventh Framework Program European Union Grant 223276 "NeuroGSK3" (to H. E.-F.) and by Alzheimer's Association Grant NIRG-11-205535 (to D. F.).

<sup>1</sup> These authors contributed equally to this work. Submitted in partial fulfillment of the requirements for a Ph.D. degree at Tel Aviv University.

<sup>2</sup> To whom correspondence may be addressed: Department of Neurobiology, George S. Wise Faculty of Life Sciences, Tel Aviv University, Tel Aviv, Israel. Fax: 972-3-640-9028; E-mail: dfrenkel@post.tau.ac.il.

<sup>3</sup> To whom correspondence may be addressed: Dept. of Human Molecular Genetics and Biochemistry, Sackler School of Medicine, Tel Aviv University, Tel Aviv 69978, Israel. Fax: 972-3-640-8749; E-mail: heldar@post.tau.ac.il.

<sup>4</sup> The abbreviations used are: A $\beta$ , amyloid  $\beta$ ; GSK-3, glycogen synthase kinase-3; mTOR, mammalian target of rapamycin; AD, Alzheimer disease; PS1, presenilin-1; v-ATPase, vacuolar ATPase; APP, amyloid precursor protein; CatD, cathepsin D; mCatD, mature CatD; 6-Bio, (2',3',5')-6-bromoindirubin-3'-oxime; eEF, eukaryotic elongation factor; MEF, mouse embryonic fibroblast; LC, light chain.

nents such as microtubule-associated protein Tau, presenilins, collapsin response mediator proteins, and  $\beta$ -catenin by GSK-3 underlie mechanisms contributing to pathogenesis (8–11), and thus inhibition of GSK-3 should be an effective therapeutic strategy (13).

The contribution of GSK-3 to A $\beta$  neuropathology has been disputed, however. Initially, it was shown that GSK-3 $\alpha$  enhanced  $\gamma$ -secretase-mediated A $\beta$  peptide production in CHO cells overexpressing APP (14). A recent report challenged these results and showed that knock-out of GSK-3 $\alpha$  or GSK-3 $\beta$  in the mouse brain did not alter levels of APP metabolites or A $\beta$  peptides (15). Other studies showed that treatment with GSK-3 inhibitors, lithium, or NP12 or silencing of GSK-3 $\alpha$  with hairpin RNA constructs reduced A $\beta$  deposition in various AD mouse models (14, 16, 17), yet our understanding of mechanisms behind GSK-3 regulation of A $\beta$  pathology is limited.

The mammalian target of rapamycin (mTOR) is a major nutrient-sensing component that integrates input from growth factors and nutrients to control cell growth (18–20). Abnormal activation of the mTOR signaling pathway has been implicated in A $\beta$  pathology and behavior dysfunctions (21, 22). Recent studies indicate a tight link between mTOR and the lysosomal system in regulating cellular responses to multiple nutrient cues (23, 24). Lysosomes are acidic organelles responsible for cellular degradation (25), and malfunction of lysosomes is causative in AD pathogenesis (26–28). Although GSK-3 may be involved in activation of mTOR (29, 30), the molecular interplay between GSK-3, lysosomal regulation, and mTOR is unknown. Nor is it known whether the GSK-3/mTOR/lysosomal axis contributes to AD pathogenesis.

To gain further insights into the role of GSK-3 in A $\beta$  pathology, we used 5XFAD mice. These mice co-express a total of five familial AD mutations in APP and presenilin-1 (PS1) and develop massive cerebral A $\beta_{42}$  loads, memory deficits, and neuron loss at an early age (31). We treated the mice nasally with L803-mts, a selective, substrate-competitive inhibitor of GSK-3 that was previously characterized in diverse biological systems (32–37). Treatment with L803-mts reduced A $\beta$  pathology and ameliorated cognitive deficits in the 5XFAD mice. By analyses of 5XFAD brains and cell-based systems, we uncovered a novel role for GSK-3 in regulating lysosomal acidification. Our data suggest that restoration of lysosomal acidification and mTOR activity is the molecular basis of the reversal in AD symptoms achieved with GSK-3 inhibition.

### EXPERIMENTAL PROCEDURES

**Materials**—L803-mts peptide was synthesized by Genemed Synthesis, Inc. AR-A014418, SB-216763, and 6-Bio were purchased from Sigma. Antibodies against phospho-GSK-3 $\alpha/\beta$ , phospho-S6K-1 (Thr-389), S6K-1, phospho-S6 (Ser-240/244), S6 protein, phospho-eukaryotic elongation factor 2 (eEF2; Thr-56), eEF2, and LC3I/II were from Cell Signaling Technologies. Antibodies against GSK-3 $\alpha/\beta$ ,  $\beta$ -actin, v-ATPase V0A1, cathepsin D, Lamp1, and Lamp2 were from Santa Cruz Biotechnology, and anti-mTOR was from Abcam. Anti-p62/SQSTM1 was from MBL. Anti- $\beta$ -catenin was from Transduction Laboratories, and anti- $\beta$ -amyloid, 1–16 (6E10) was purchased from Covance.

**Animals and Behavior Tests**—We used 5XFAD transgenic mice (Tg6799) that co-overexpress FAD mutant forms of human APP (the Swedish mutation, K670N/M671L; the Florida mutation, I716V; and the London mutation, V717I) and PS1 (M146L/L286V) transgenes under transcriptional control of the neuron-specific mouse Thy-1 promoter (31). Hemizygous transgenic mice were crossed with C57Bl/6J breeders. Genotyping was performed by PCR analysis of tail DNA as described (31). The mice were housed in individual cages in a temperature-controlled facility with a 12-h light/dark cycle. 5XFAD mice were randomly assigned to two groups (six animals each). Treatment started at the age of 2 months, and L803-mts (80  $\mu$ g total in vehicle solution, 128 mM NaCl, 8 mM citric acid monohydrate, 17 mM disodium phosphate dehydrate, and 0.0005% benzalkonium chloride) was administered intranasally (5  $\mu$ l of solution in each nostril) every other day for 120 days. The contextual fear conditioning test was conducted as described (38). Briefly, mice were subjected to an unconditioned electric stimulus (one foot shock; 1 s/1 mA) in a training pre-session. 24 h later, a fear conditioning test was performed by scoring freezing behavior, e.g., the absence of all but respiratory movement for 180 s using a FreezeFrame automated scoring system (Coulbourn Instruments). All experiments were in compliance with protocols approved by the Tel Aviv University animal care committee.

**Histology and A $\beta$  Staining**—Saline-perfused brains were rapidly excised and frozen in N<sub>2</sub>. The brains were divided into the two hemispheres: the left hemisphere was taken for immunohistology, and the right hemisphere was taken for immunoblot analysis. Coronal brain sections (14  $\mu$ m) were cut by cryostat at  $-20$  °C. Slices at Bregma  $-1.58$  mm were fixed (4% paraformaldehyde) and stained with Congo red dye (Sigma-Aldrich) or with an antigen-retrieval method with anti-A $\beta$  6E10 antibody (SIG-39300) and visualized by fluorescence microscopy. Quantification of A $\beta$  depositions was done for the whole hippocampus area in a blinded fashion using Imaging Research software from the National Institutes of Health in an unbiased stereological approach.

**Brain Extracts**—Right cerebral hemispheres were homogenized in ice-cold buffer H (150 mM  $\beta$ -glycerophosphate, pH 7.3, 10% glycerol, 5 mM EGTA, 5 mM EDTA, 40 mM NaF, 25 mM sodium pyrophosphate, 25  $\mu$ g/ml leupeptin, 25  $\mu$ g/ml aprotinin, 10  $\mu$ g/ml pepstatin A, 1 mM DTT, and 1% Nonidet P-40). The extracts were centrifuged at 14,000  $\times g$  for 30 min, and supernatants were collected. Equal amounts of protein (30–50  $\mu$ g) were subjected to gel electrophoresis followed by immunoblot analysis using the indicated antibodies. Analysis of  $\beta$ -actin levels demonstrated equal protein loading.

**Cell Culture and Transfection**—SH-SY5Y cells were grown in RPMI 1640 medium supplemented with 10% FCS, 5 mM L-glutamine, and 0.04% gentamycin. The cells were maintained in growth medium, in RPMI supplemented with 0.1% or 1.5% FCS, or in a Krebs-Ringer-HEPES buffer (12 mM NaCl, 0.4 mM KH<sub>2</sub>PO<sub>4</sub>, 0.1 mM MgSO<sub>4</sub>, 0.1 mM CaCl<sub>2</sub>, 1 mM NaHCO<sub>3</sub>, 3 mM HEPES, pH 7.4, and 11 mM glucose) supplemented with 0.1% FCS. The cells were treated with L803-mts (40  $\mu$ M), AR-A014418 (20  $\mu$ M), SB-216763 (10  $\mu$ M), 6-Bio (5  $\mu$ M), chloroquine (30  $\mu$ M), or rapamycin (50 nM) for 5 h or with tunica-

mycin (5  $\mu\text{g}/\text{ml}$ ) for 2 h. Mouse embryonic fibroblast cells deficient in presenilin 1 and presenilin 2 (MEF-PS1/2<sup>-/-</sup>) were generously provided by Dr. Bart De Strooper (KU Leuven University, Leuven, Belgium) (39). The cells were grown in DMEM supplemented with 10% FCS, 5 mM L-glutamine, and 1% penicillin-streptomycin. Chinese hamster ovary cells stably expressing human wild-type APP-751 (CHO-APP) were kindly provided by Dr. Denis Selkoe (Harvard Medical School) and were grown in DMEM/F-12 medium supplemented with 10% FCS, 2 mM L-glutamine, 0.5 mg/ml L-proline, and 1% penicillin-streptomycin and maintained with antibiotics for G418 selection (1 mg/ml). SHSY-5Y cells were transiently transfected with GFP-GSK-3 constructs (5–7  $\mu\text{g}$ ) using Lipofectamine 2000 (Invitrogen). For silencing of GSK-3, the cells were transfected with 50 nM GSK-3 $\alpha$  or GSK-3 $\beta$  siRNA or with a scrambled control siRNA (Thermo Scientific/Dharmacon) using the transfection reagent Dharmafect (Thermo Scientific/Dharmacon) according to the manufacturer's instructions. For infections, we used recombinant adenovirus coding for GSK-3 $\alpha$  or GSK-3 $\beta$  (prepared by Z. Liberman in the laboratory) at 1:500 dilution. Adenovirus coding for  $\beta$ -gal was used as a control. The cells were harvested 24 h postinfection.

**Partial Purification of Lysosomes**—The cells were washed with PBS, collected with wash buffer (125 mM KCl, 30 mM Tris, pH 7.5, 5 mM MgOAc, 1 mM  $\beta$ -mercaptoethanol), and centrifuged at  $800 \times g$  for 5 min. The cells were resuspended in hypotonic buffer (10 mM KCl, 30 mM Tris, pH 7.5, 5 mM MgOAc, 1 mM  $\beta$ -mercaptoethanol, and protease inhibitors aprotinin, leupeptin, and pepstatin A) and broken by 30 piston strokes. Homogenates were centrifuged at  $1000 \times g$  to precipitate nuclei. The supernatants were collected and centrifuged at  $100,000 \times g$  for 1 h at 4 °C. The particulate membrane fraction that included lysosomes was boiled with SDS sample buffer and subjected to immunoblot analysis. Detection of Lamp1 in the pellet and not in the supernatant confirmed the presence of lysosomes in this fraction.

**Gel Electrophoresis and Immunoblotting**—The cells were collected and lysed in an ice-cold buffer G (20 mM Tris-HCl, 10% glycerol, 1 mM EDTA, 1 mM EGTA, 0.5% Triton X-100, 0.5 mM orthovanadate, 10 mM  $\beta$ -glycerophosphate, 5 mM sodium pyrophosphate, 50 mM NaF, 1 mM benzaminidine, and protease inhibitors aprotinin, leupeptin, and pepstatin A). Cell extracts were centrifuged at  $14,000 \times g$  for 20 min, and supernatants were collected. Equal amounts of protein (40  $\mu\text{g}$ ) were subjected to gel electrophoresis and Western blot analysis using indicated antibodies. Analysis of  $\beta$ -actin levels demonstrated equal protein loading.

**Live Cell Imaging**—The cells were treated as indicated and incubated with 75 nM LysoTracker Red (Molecular Probes) for 30 min at 37 °C. Live cell imaging was taken using a  $63.0 \times 1.40$  oil UV objective lens on a laser scanning confocal microscope (Leica TCS-SP5 II) with spatial resolution of 50–70 nm. Z-projection images were collected, and stacked images (23 stacks) were generated using LAS-AF Lite software.

**Statistical Analysis**—Data comparisons were performed using the Student's *t* test when two groups were compared or one-way analysis of variance when three or more groups were analyzed.

## RESULTS

**L803-mts Treatment Reduces A $\beta$  Deposits and Ameliorates Cognitive Deficits in 5XFAD Mice**—We first compared GSK-3 levels in hemi-brain blots prepared from 5XFAD mice and age-matched C57Bl/6J mice of similar genetic background (referred to here as wild type (WT)). GSK-3 $\alpha$  and GSK-3 $\beta$  protein levels were comparable in WT and 5XFAD mice; however, phosphorylation levels on serine inhibitory sites (Ser-21 on GSK-3 $\alpha$  and Ser-9 on GSK-3 $\beta$ ) were markedly lower in the 5XFAD brains than in WT brains (Fig. 1A), indicating that both GSK-3 isozymes are hyperactive in the 5XFAD brain.

The 5XFAD mice begin to develop amyloid plaque burdens at 2 months of age (31). Therefore, L803-mts treatment was begun at 2 months of age, and the compound was given nasally for 120 days. We chose the nasal route because this has previously been demonstrated to be an effective drug delivery route to the central nervous system (40, 41). Increased levels in brain  $\beta$ -catenin served as an *in vivo* marker for inhibition of GSK-3 by L803-mts (Fig. 1B), because GSK-3 activity destabilizes  $\beta$ -catenin (42, 43). Interestingly, in untreated mice,  $\beta$ -catenin levels were lower in 5XFAD brains than in WT brains (Fig. 1B), a possible outcome of hyperactive GSK-3 (Fig. 1A) and a phenomenon detected in AD patients carrying the PS1 mutation (44). At 6 months of age, mice were subjected to a contextual fear conditioning test, a behavioral test widely used to evaluate associative learning and memory. As reported previously, untreated 5XFAD mice showed poorer cognitive abilities than WT mice (31, 45), manifested by reduced freezing duration ( $20 \pm 10\%$  of the time of WT mice; Fig. 1C). Treatment with L803-mts improved performance to  $72 \pm 14\%$  of WT mice (Fig. 1C).

We then analyzed the impact of L803-mts on A $\beta$  loads. Treatment with L803-mts reduced the amount and the mean sizes of A $\beta$  loads by  $75 \pm 6.8\%$  as evaluated by staining of brain sections with Congo red dye (Fig. 1D, upper panels). This was further confirmed by immunostaining of brain sections with a specific A $\beta$  monoclonal antibody that indicated a reduction in A $\beta$  loads by  $84 \pm 20\%$  (Fig. 1D, lower panels). Because intraneuronal A $\beta_{42}$  is the primary peptide that accumulates in this model (31), it appeared that L803-mts treatment significantly reduced levels of this A $\beta$  species. Total APP holoprotein levels were not reduced by L803-mts (Fig. 1E), suggesting that the effect on A $\beta$  loads is post-translational. Thus, inhibition of GSK-3 by L803-mts attenuated the progressive accumulation of A $\beta$  deposits in the mouse brain and improved cognitive functions.

**L803-mts Inhibits Autophagy and Restores mTOR and Lysosomal Activity in the 5XFAD Brain**—We next sought to investigate the mechanism of action responsible for reduction in A $\beta$  pathology upon inhibition of GSK-3. Levels of insulin-degrading enzyme, an enzyme that degrades A $\beta$  plaques (46), were not altered by treatment with L803-mts (Fig. 2A), nor did we find changes in the expression levels of the chaperone heat shock protein (Hsp70) or defects in the insulin signaling pathway (as demonstrated by phosphorylation of Akt/PKB) (Fig. 2A), both implicated in protein aggregate degradation (47–49). It should be noted that GSK-3 is phosphorylated by multiple protein

## GSK-3/Lysosomes/mTOR Axis in the Alzheimer Disease Brain

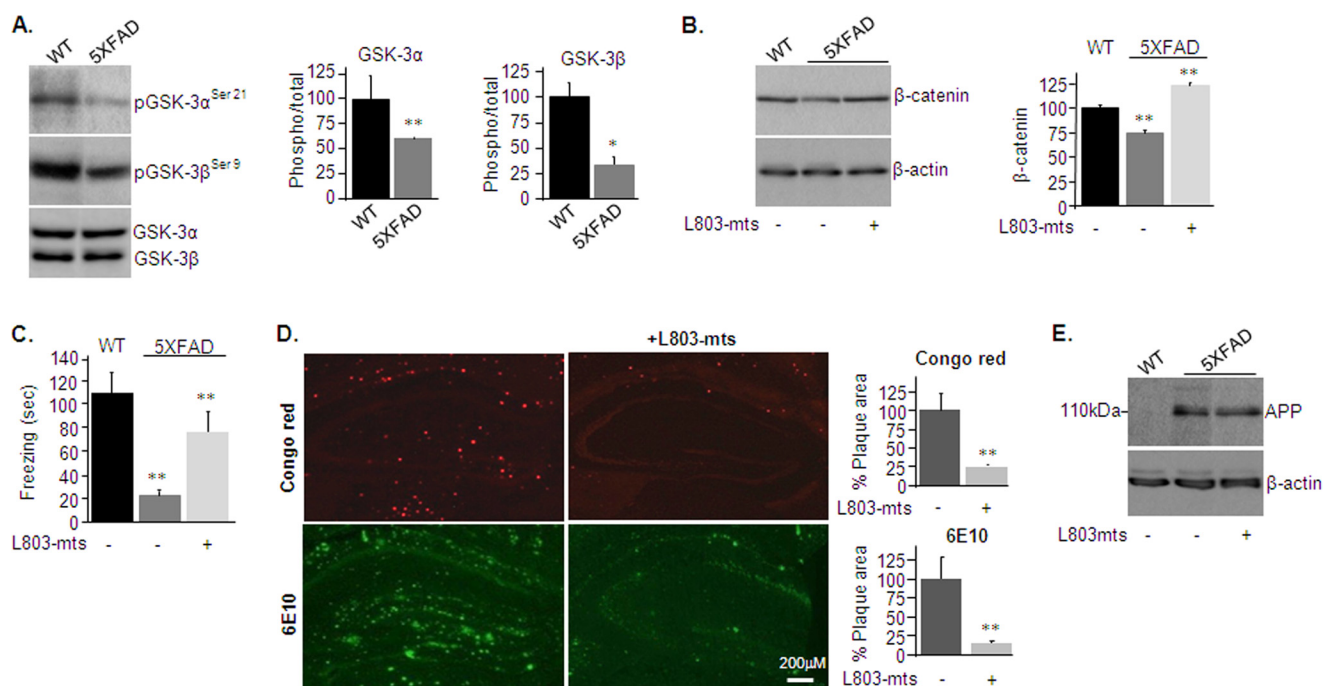


**FIGURE 1. L803-mts reduces A $\beta$  plaque loads and improves cognitive performance in the 5XFAD mouse model.** *A*, phosphorylation and expression levels of GSK-3 $\alpha$ / $\beta$  in brain samples of WT and 5XFAD mice as determined by immunoblot analysis. *B*,  $\beta$ -catenin levels in brain samples from WT and L803-mts-treated or nontreated 5XFAD mice as determined by immunoblot analysis. Densitometry analyses of indicated bands or calculated ratios are shown on the *right* for each panel. *C*, freezing time duration determined in WT mice and in L803-mts-treated or nontreated 5XFAD mice, as evaluated in the contextual fear conditioning test. *D*, representative histological images of paraformaldehyde-fixed hemi-brain sections obtained from L803-mts-treated or nontreated 5XFAD mice. The *upper panels* show a Congo red stain, and the *lower panels* show an immunostaining using anti-A $\beta$  antibody (6E10). The percentage of plaque load area is shown on the *right*. *E*, expression levels of APP in brain samples from WT and L803-mts-treated or nontreated 5XFAD mice as determined by immunoblot analysis. Densitometry analyses for all panels are the means  $\pm$  S.E. of five or six animals. \*,  $p < 0.05$ ; \*\*,  $p < 0.005$ . Equal protein loads were verified by  $\beta$ -actin blots (*B* and *E*).

kinases other than Akt, including Ca<sup>2+</sup> calmodulin-dependent protein kinase II, PKA, and S6 ribosomal proteins kinase p90 RSK (50–52). In addition, GSK-3 is dephosphorylated by several different phosphatases (53). Thus, alterations in GSK-3 phosphorylation observed in the 5XFAD brain (Fig. 1*A*) could be catalyzed by one or more of these components.

We thus considered mechanisms mediated by the autophagy/lysosomal degradative pathway that recycles macromolecules and organelles (54, 55). This pathway was recently implicated in APP processing and A $\beta$  clearance (27, 56). LC3-II, a lipidated form of microtubule-associated protein 1 light chain 3-I (LC3-I), is exclusively associated with autophagosomal membranes and serves as a marker for autophagosomes (54, 57, 58). Levels of LC3-II and the relative ratio of LC3-II to total LC3 (LC3-I+LC3-II) were similar in 5XFAD and WT brains as determined by immunoblot analysis (Fig. 2*B*). Treatment with L803-mts led to a small reduction in LC3-II/LC3 ratio (Fig. 2*B*), indicating that L803-mts could inhibit autophagy. To support this possibility, we measured p62/SQSTM1, an autophagy substrate whose levels inversely correlate with autophagic activity (59). Indeed, treatment with L803-mts significantly increased p62/SQSTM1 levels in the 5XFAD mouse brain (Fig. 2*C*), indicating that L803-mts inhibited autophagic activity.

The mTOR is a “classical” autophagy suppressor (54, 60, 61). We thus sought to determine whether mTOR activity was altered by in L803-mts-treated mice. mTOR activity was evaluated by measuring the phosphorylation levels of the direct mTOR target p70S6 ribosomal kinase (S6K1) and its down-

stream substrate ribosomal S6 protein (S6). We also determined the phosphorylation levels of eEF2, an essential factor in the protein synthesis machinery and a downstream target of mTOR (62) and GSK-3 (29). Phosphorylation of eEF-2 on Thr-56 inhibits its activity (62). Phosphorylation levels of S6K1 and S6 were significantly reduced in 5XFAD brains as compared with WT brains (Fig. 2*D*), and treatment with L803-mts enhanced phosphorylation of these proteins in brains of 5XFAD mice (Fig. 2*D*). In addition, phosphorylation of eEF-2 was reduced in L803-mts-treated 5XFAD brains, indicating activation of eEF-2 (Fig. 2*D*). Together, these data indicated that L803-mts restored mTOR activity, which was inhibited in the 5XFAD mice brain.

We next examined the activity of the lysosomal pathway that may clear aggregated proteins, including A $\beta$  loads, independent of autophagy (26, 28, 63). Lysosomes are acidic organelles that contain many hydrolytic enzymes (64, 65). The vacuolar ATPase (v-ATPase) proton pump maintains lysosomal acidification (66, 67). Cathepsin D (CatD), the principal lysosomal aspartyl protease, is highly abundant in the brain and activated by proteolysis in the acidified lysosome to produce a mature proteolytic product (mCatD) (68). Precursors CatD (~46–52 kDa) and mCatD (~32 kDa) were detected in WT, L803-mts treated, and nontreated 5XFAD brains (Fig. 3*A*). mCatD levels were lower in the 5XFAD brains than in WT brains, and treatment with L803-mts restored this deficit (Fig. 3*A*). These results indicated that lysosomal acidification is impaired in the 5XFAD brains. To further assess lysosomal acidification, we

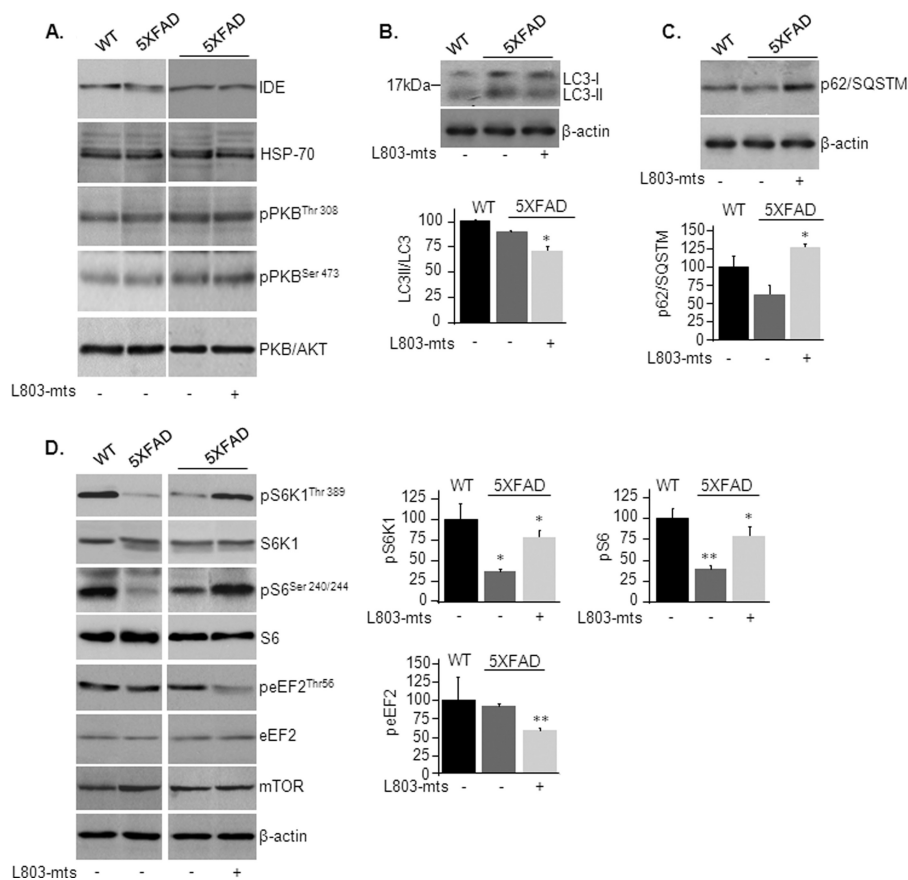


**FIGURE 2. L803-mts reactivates mTOR and inhibits autophagy in the 5XFAD mice.** *A*, phosphorylation and/or expression levels of insulin-degrading enzyme (*IDE*), Hsp70, and AKT/PKB in brain samples from WT and L803-mts-treated or nontreated 5XFAD mice as determined by immunoblot analysis. *B*, LC3-I and LC3-II levels in brain samples from WT and L803-mts-treated or nontreated 5XFAD mice as determined by immunoblot analysis. Calculated ratios of LC3-II/total LC3 are shown in the *lower panel*. *C*, levels of p62/SQSTM1 in brain samples from WT and L803-mts-treated or nontreated 5XFAD mice as determined by immunoblot analysis. Densitometry analyses are shown in the *lower panel*. *D*, phosphorylation of mTOR targets S6K1, S6, and eEF2 in brain samples from WT and L803-mts-treated or nontreated 5XFAD mice as determined by immunoblot analysis. Expression of total protein and total mTOR is also shown. Densitometry analyses of indicated bands are shown on the *right*. For all panels, the results are the means  $\pm$  S.E. of five or six animals. \*,  $p < 0.05$ ; \*\*,  $p < 0.005$ . Equal protein loads were verified by  $\beta$ -actin blots (*B–D*).

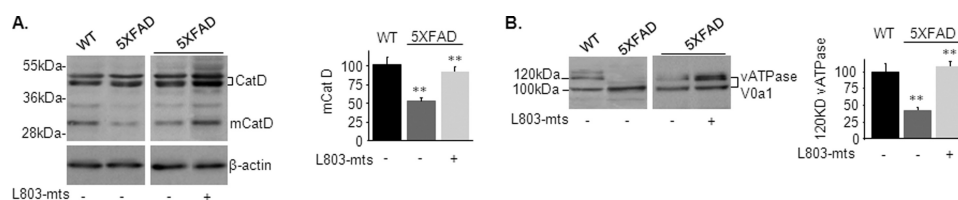


**FIGURE 3. L803-mts restores impaired lysosomal acidification in the 5XFAD mouse brain.** *A*, levels of precursor CatD (~46–52 kDa) and the proteolytic product mCatD (~32 kDa) in brain samples from WT and L803-mts-treated or nontreated 5XFAD mice as determined by immunoblot analysis.  $\beta$ -Actin levels are also shown. *B*, glycosylated (120 kDa) and nonglycosylated (100 kDa) v-ATPase V0a1 in brain samples from WT and L803-mts-treated or nontreated 5XFAD mice as determined by immunoblot analysis. Densitometry analysis of indicated proteins is shown on the *right* of each panel. The results are the means  $\pm$  S.E. of five or six animals. \*,  $p < 0.05$ ; \*\*,  $p < 0.005$ .

determined the extent of *N*-glycosylation of the v-ATPase subunit, ATPase V0a1, that facilitates assembly of the proton pump in the lysosome (69, 70). Immunoblot analysis using anti-v-ATPase V0a1 antibody revealed a doublet band corresponding to nonglycosylated (100 kDa) and mature glycosylated (120 kDa) v-ATPase V0a1 in brains of all groups (Fig. 3*B*). Levels of mature ATPase V0a1 were lower in the 5XFAD brains than in WT brains (Fig. 3*B*), and treatment with L803-mts increased mature ATPase V0a1 levels by 2.5-fold (Fig. 3*B*). Therefore, one of the effects of GSK-3 inhibition by L803-mts is to restore lysosomal acidification in the 5XFAD brain by facilitating *N*-glycosylation of v-ATPase V0A1.

**Role of GSK-3 in Regulating Lysosomal Acidity**—We next used a simple cell culture system to validate our *in vivo* results and to gain further insights into GSK-3 regulation of lysosomes and mTOR. Treatment of “neuron-like” human neuroblastoma SH-SY5Y cells with L803-mts activated lysosomal proteolytic activity as determined by increased levels of mCatD in “total” cell extract (Fig. 4*A*) or in partially purified lysosomes (data not shown). Treatment with chloroquine, which neutralizes lysosomal pH, served as a negative control and lowered mCatD (Fig. 4*A*). An increase in glycosylated v-ATPase V0a1 (Fig. 4*B*) further indicated that L803-mts treatment enhanced lysosomal acidification. Treatment with tunicamycin, which blocks

## GSK-3/Lysosomes/mTOR Axis in the Alzheimer Disease Brain

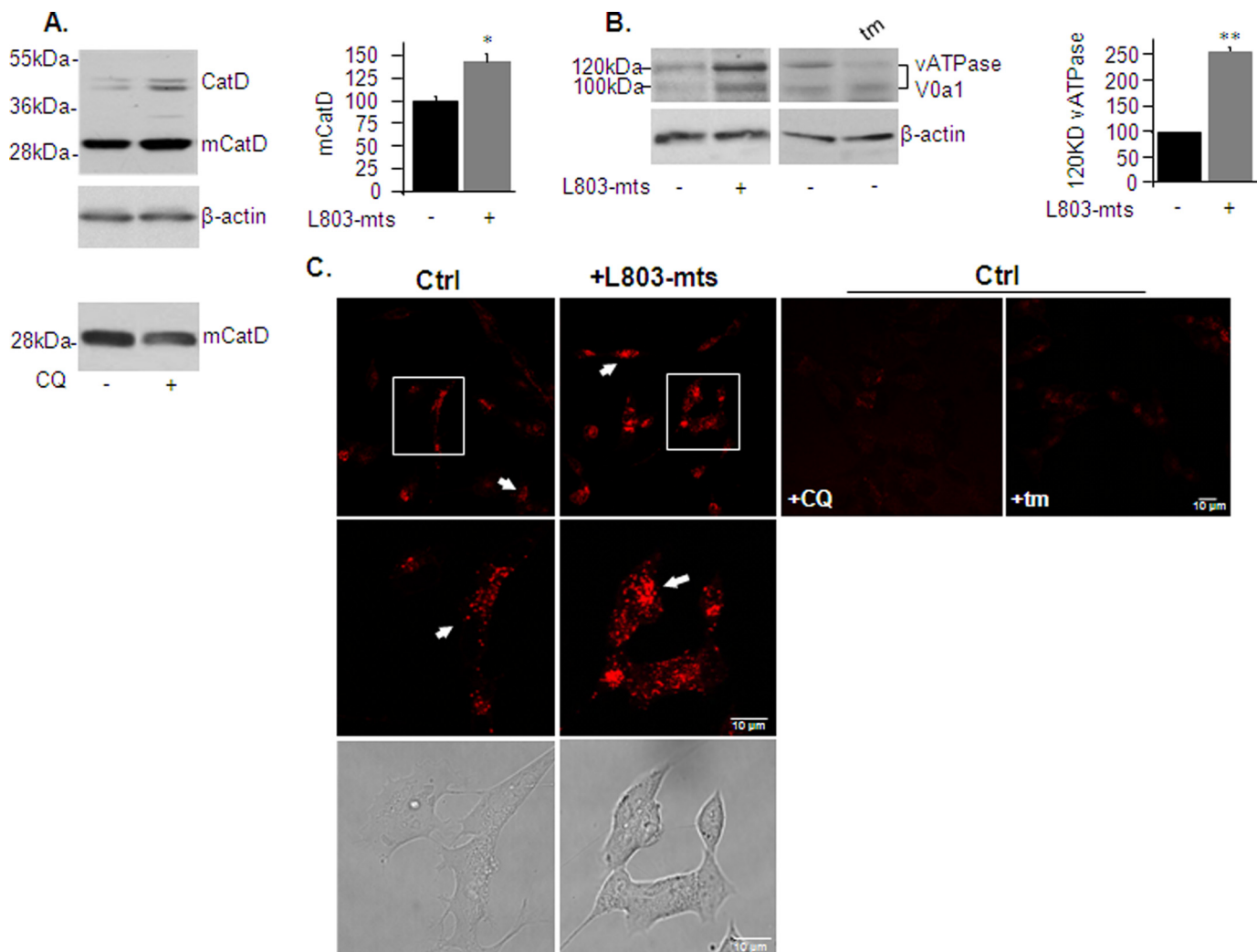


**FIGURE 4. L803-mts increases lysosomal acidification in SHSY-5Y cells.** *A*, SHSY-5Y cells were treated with L803-mts (40  $\mu$ M, 5 h), and the levels of CatD (~46–52 kDa) and mCatD (~32 kDa) were determined by immunoblot analysis. Treatment of cells with chloroquine (CQ) (30  $\mu$ M, 3 h) is shown in the *bottom panel*. The  $\beta$ -actin levels are also shown. *B*, SHSY-5Y cells were treated as in *A* or treated with tunicamycin (tm) (5  $\mu$ g/ml, 2 h). Levels of glycosylated or nonglycosylated v-ATPase V0a1 were determined by immunoblot analysis. The  $\beta$ -actin levels are also shown. Densitometry analysis of indicated proteins is shown on the *right*. The results are the means of three independent experiments  $\pm$  S.E. \*  $p < 0.05$ ; \*\*  $p < 0.005$ . *C*, SHSY-5Y cells were treated with L803-mts, chloroquine (CQ), or tunicamycin (tm) as described. The cells were stained with LysoTracker Red (Lys) and imaged by confocal microscopy. *White arrows* mark lysosomal red vesicles (*top panels*). Zooms of the *boxed areas* in the *top panels* are shown in the *middle panels*. Bright filled cell images are shown in the *bottom panels*. The fluorescence images present Z-projection image stacks (23 images). *Scale bars* represent 10  $\mu$ m. *Ctrl*, control.

*N*-linked glycosylation of proteins, abolished the 120-kDa band of v-ATPase V0a1 and verified glycosylation (Fig. 4*B*).

We examined changes in lysosomal acidity using LysoTracker Red, a dye that accumulates in acidic organelles. The cells were stained with LysoTracker Red, and live cells were imaged by confocal microscopy. Lysosomes appeared as red punctate in cell images (Fig. 4*C*). Treatment with chloroquine reduced the fluorescence of the red vesicles and confirmed dye specificity (Fig. 4*C*). A similar observation was obtained after treatment with tunicamycin, verifying the importance of glycosylation in lysosomal acidification (Fig. 4*C*). Treatment of cells with L803-mts increased the number of acidified lysosomes and intensity of staining as compared with control untreated cells (Fig. 4*C*). These results were consistent with the *in vivo* data and indicate that L803-mts increased the pool of acidic lysosomes.

To examine whether GSK-3 isozymes have distinct roles in regulating lysosomal acidity (and activity), GSK-3 $\alpha$  or GSK-3 $\beta$  were overexpressed in SH-SY5Y cells using a recombinant ade-

novirus system. Control cells were infected with  $\beta$ -gal adenovirus. Overexpression of either GSK-3 $\alpha$  or GSK-3 $\beta$  markedly reduced mCatD levels (Fig. 5*A*). We next evaluated the effect of inhibition of GSK-3 expression using siRNA. Although the reduction in GSK-3 $\beta$  expression increased mCatD levels (Fig. 5*B*), silencing of GSK-3 $\alpha$  had no significant effects (Fig. 5*B*). It is possible that reductions in GSK-3 $\alpha$  levels were not sufficient to impact lysosomal acidification or that activity of GSK-3 $\beta$  compensated for the reduction in GSK-3 $\alpha$  activity. The cells were then transfected with GFP-tagged-GSK-3 $\alpha$  or -GSK-3 $\beta$  and were stained with LysoTracker Red. Staining was consistently lower in cells expressing the GSK-3 isozymes as compared with control cells expressing the GFP protein only (Fig. 5*C*). Levels of lysosomal Lamp2 were not significantly altered in the GSK-3 overexpressing cells (Fig. 5*D*), indicating that GSK-3 did not affect lysosomes number but, rather, altered their acidification. We concluded that both GSK-3 isozymes impair lysosomal acidification.

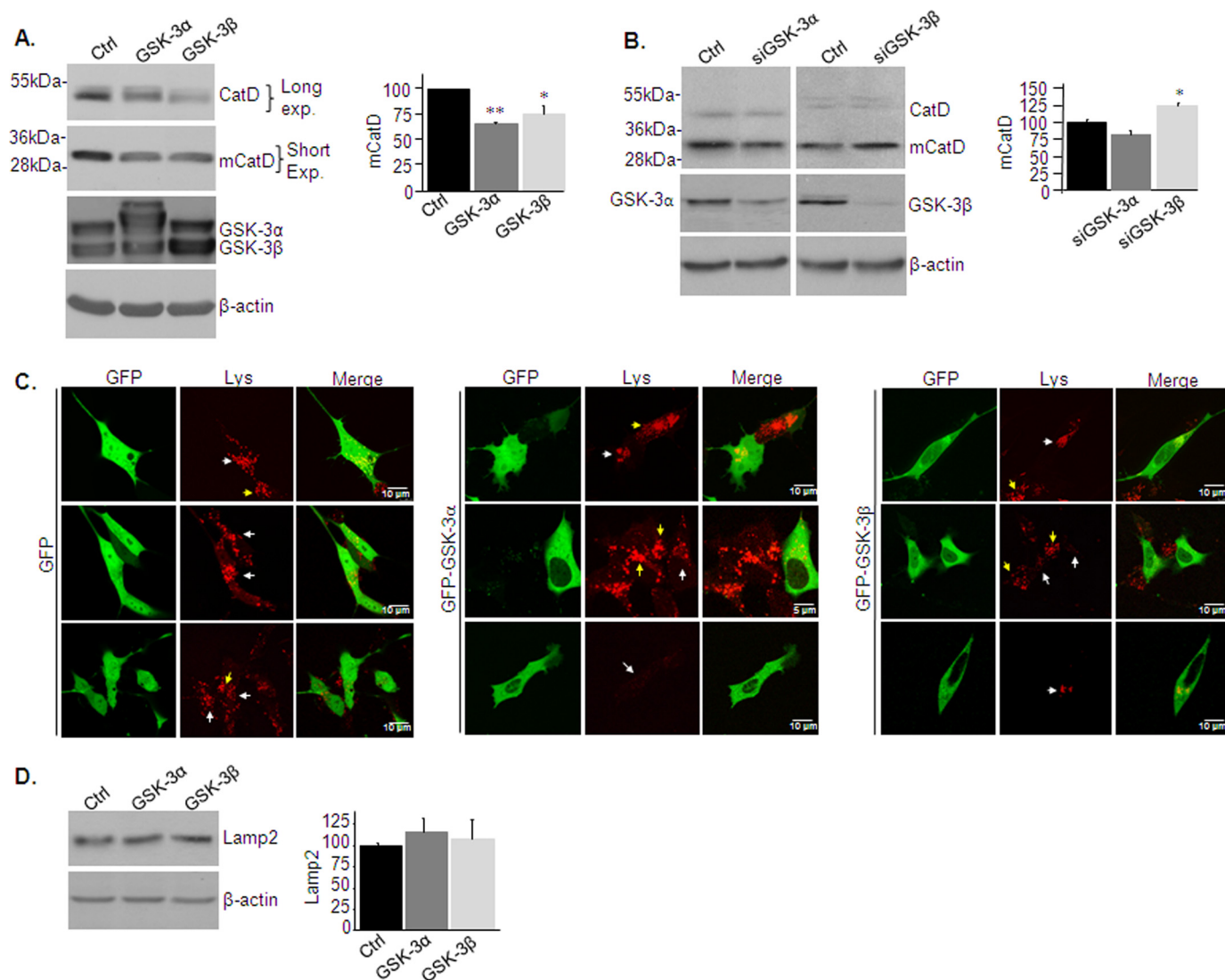


**FIGURE 5. GSK-3 impairs lysosomal acidification in SHSY-5Y cells.** *A*, SHSY-5Y cells were infected with adenovirus coding for GSK-3 $\alpha$  or GSK-3 $\beta$ . The levels of CatD (~46–52 kDa) and mCatD (~32 kDa) were determined by immunoblot analysis. Long and short exposures are shown to allow detection of CatD and mCatD within the linear range. Control cells were infected with a  $\beta$ -gal-coding adenovirus (*Ctrl*). Expression of GSK-3 $\alpha/\beta$  are shown in the *middle* and *right* panels. *B*, SHSY-5Y cells were transfected with siRNA targeting GSK-3 $\alpha$  or GSK-3 $\beta$ . The levels of CatD (~46–52 kDa) and mCatD (~32 kDa) were determined by immunoblot analysis. Control cells were transfected with scrambled control siRNA (*Ctrl*). Densitometry analysis of indicated proteins is shown on the *right* of each panel. The results are the means of three independent experiments  $\pm$  S.E. \* $p$  < 0.05; \*\* $p$  < 0.005. *C*, SH-SY5Y cells were transfected with GFP-GSK-3 $\alpha$  or GFP-GSK-3 $\beta$  constructs. Control cells were transfected with a GFP coding construct. The cells were stained with LysoTracker Red (Lys) and imaged by confocal microscopy. Representative images are shown as indicated. The *arrows* indicate acidic lysosomes in the transfected cells (*white arrows*) or in the nontransfected cells (*yellow arrows*). The fluorescence images in the *top* panels represent Z-projection image stacks (23 images). The *scale bars* represent 5 or 10  $\mu$ m. *D*, levels of Lamp2 were determined in cells from *C*. Equal protein loads were verified by  $\beta$ -actin blots (*A*, *B*, and *D*).

*mTOR Is Activated by GSK-3 and Inhibited by Impaired Lysosomal Activity or Overexpression of APP*—Our *in vivo* results indicated that treatment with L803-mts restored mTOR activity in the 5XFAD brain (Fig. 2D). It may be that hyperactive GSK-3 in the 5XFAD brain (Fig. 1A) is responsible for inhibition in mTOR. We evaluated the regulation of mTOR by GSK-3 in SH-SY5Y cells. Overexpression of GSK-3 $\alpha$  or GSK-3 $\beta$  in these cells activated mTOR as indicated by increased phosphorylation of the mTOR targets S6K1 and S6 (Fig. 6A). The use of rapamycin, which primarily blocks activity of the mTORC1 complex, suggested that GSK-3 activates mTORC1 (Fig. 6B). Treatment with diverse GSK-3 inhibitors SB-216763, CT-99012, 6-Bio, and L803-mts verified this conclusion; all inhibitors inhibited the phosphorylation of S6 (Fig. 6C). Hence,

reactivation of mTOR observed in L803-mts-treated 5XFAD mice was likely not a direct consequence of inhibition of GSK-3, nor was hyperactivity of GSK-3 responsible for the inhibition of mTOR detected in 5XFAD brains.

We thus searched for additional elements that could inhibit mTOR in the 5XFAD brain. We examined whether defective lysosomal acidification inhibit mTOR. Indeed, treating cells with chloroquine reduced phosphorylation of S6 (Fig. 6D). Overexpression of GSK-3 $\alpha$  or GSK-3 $\beta$  prevented (in part) inhibition in mTOR by chloroquine (Fig. 6D). Hence, GSK-3 activates mTOR independent of lysosomal acidity. We also considered that elevated burdens of APP or A $\beta$  may inhibit mTOR in the 5XFAD brain. We thus examined mTOR activity in Chinese hamster ovary cells stably expressing APP (CHO-APP<sub>751</sub>).

## GSK-3/Lysosomes/mTOR Axis in the Alzheimer Disease Brain

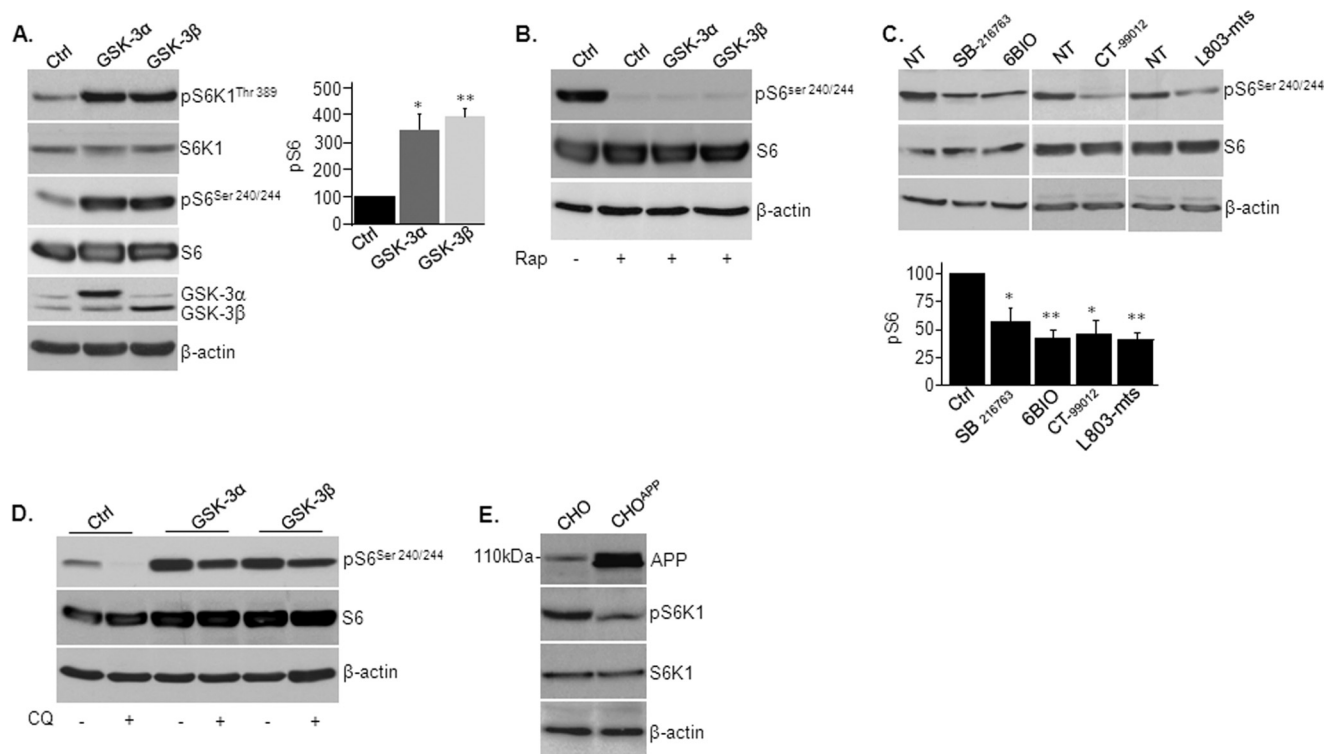


**FIGURE 6. Regulation of mTOR activity by GSK-3, lysosomes, and APP.** A, SHSY-5Y cells were infected with adenovirus coding for GSK-3 $\alpha$  or GSK-3 $\beta$ . Phosphorylation levels of indicated mTOR targets were determined by immunoblot analysis. Densitometry analysis of indicated proteins is shown at the right. B, SHSY-5Y cells were infected with adenovirus coding for GSK-3 $\alpha$  or GSK-3 $\beta$  and were treated with rapamycin (*Rap*) (50 nM, 2 h). Phosphorylation levels of S6 were determined by immunoblot analysis. Control cells (*Ctrl*) were infected with a  $\beta$ -gal coding adenovirus. C, SHSY-5Y cells were treated with GSK-3 inhibitors SB-216763 (10  $\mu$ M), CT-99012 (20  $\mu$ M), 6-Bio (5  $\mu$ M), and L803-mts (40  $\mu$ M) for 5 h. The phosphorylation levels of S6 were determined by immunoblot analysis. NT, nontreated. D, SHSY-5Y cells infected with adenovirus coding for GSK-3 $\alpha$  or GSK-3 $\beta$  and were treated with chloroquine (CQ) (30  $\mu$ M, 2 h). Phosphorylation levels of S6 were determined by immunoblot analysis. E, phosphorylation levels of S6K1 were determined in CHO-APP751 and control CHO cells by immunoblot analysis. Equal protein loads were verified by  $\beta$ -actin blots.

Indeed, phosphorylation levels of mTOR targets were substantially lower in the CHO-APP<sub>751</sub> cells as compared with control CHO cells (Fig. 6E). Taken together, our data indicate that GSK-3 is a positive regulator of mTOR and suggest that defective lysosomal acidification and high APP/A $\beta$  burdens were responsible for impaired mTOR activity in the 5XFAD brain.

**L803-mts Restores Impaired Lysosomal Acidification in Cells Deficient in Presenilins**—PS1 is essential for lysosomal acidification (69, 71). Although our results implicated activation of GSK-3 as a possible mechanism responsible for impaired lysosomal acidification in the 5XFAD brain, we cannot ignore the possibility that dysfunctional PS1 is another factor that disrupts lysosomal activity. It was thus important to evaluate whether L803-mts restored lysosomal acidification caused by defective PS. For this purpose, we used MEF cells deficient in PS1 and PS2 (MEF-PS1/2<sup>-/-</sup>) (39). MEF-PS1/2<sup>-/-</sup> exhibited reduced mature ATPase V0a1, reduced mCatD levels (Fig. 7A), and less acidified lysosomes than wild-type cells (Fig. 7B). Treating MEF-PS1/2<sup>-/-</sup> cells with L803-mts increased the number and intensity of staining of lysosomes (Fig. 7B). Similar results were obtained in cells treated with different GSK-3 inhibitors, SB-216763 or LiCl (Fig. 7B). Study in partial purified lysosomes showed that L803-mts increased glycosylated content of ATPase V0a1 and increased mCatD levels but did not alter levels of Lamp1 (Fig. 7C). These data show that GSK-3 inhibition can compensate for impaired lysosomal acidification caused by dysfunctional PS1/PS2.

## DISCUSSION

In this study we showed that inhibition of GSK-3 reduced the burden of A $\beta$  plaques in an aggressive Alzheimer model, the 5XFAD mouse. We provided a proof of therapeutic benefits of nasal administration of the GSK-3 inhibitor, L803-mts, and gained new insight into the mechanisms underlying GSK-3 regulation of A $\beta$  pathology and cognition. Our data show that GSK-3 regulates lysosomal acidification and is an mTOR activator. We suggest that the molecular interplay between the lysosomal and mTOR pathways governed by GSK-3 inhibition is a molecular basis for reduced amyloid  $\beta$  pathology and improved cognition observed in the L803-mts-treated AD mice.

Our study revealed a previously unsuspected link between GSK-3 and the regulation of lysosomal function. Lysosomal acidification was impaired in the 5XFAD brain, and treatment with L803-mts restored acidification. This recovery was mediated at least in part by increased glycosylation of v-ATPase subunit V0a1; this subunit facilitates the “correct” assembly of the v-ATPase proton pump important for lysosomal acidification (69). Data from *in vitro* studies using SH-SY5Y cells supported our conclusions. Cell-based studies showed that overexpression of either GSK-3 isozyme impaired lysosomal acidification and that treatment with L803-mts enhanced CatD activity, enhanced glycosylation of V0a1, and increased the pool of acidified lysosomes. Treatment with tunicamycin confirmed the importance of glycosylation in maintaining lysosomal acidification (Fig. 4).

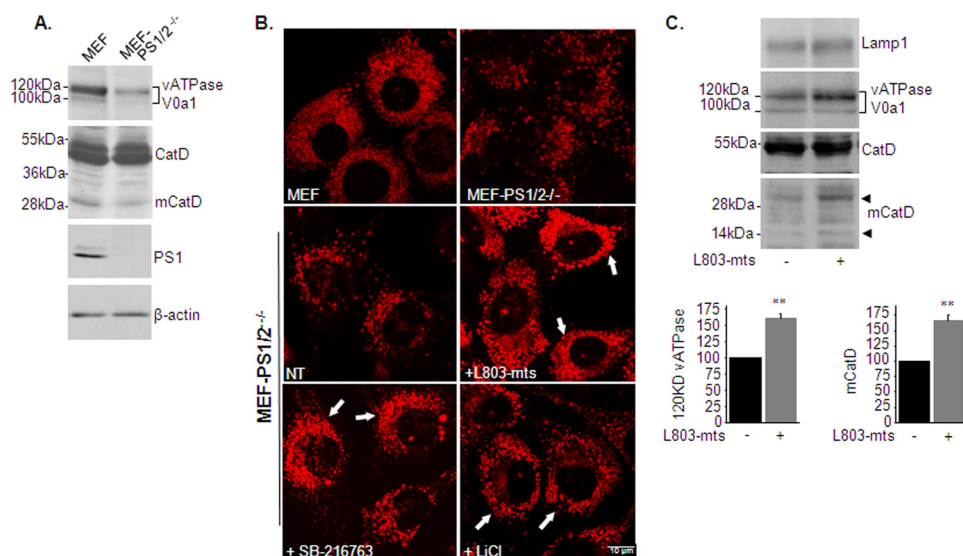


**FIGURE 7. L803-mts restores lysosomal acidification in PS1/2-deficient cells.** *A*, levels of glycosylated (120 kDa) and nonglycosylated (100 kDa) v-ATPase V0a1, CatD (~48–50 kDa), and mCatD (~32 kDa) were determined in MEF and MEF-PS1/2<sup>-/-</sup> cells by immunoblot analysis. *B*, MEF and MEF-PS1/2<sup>-/-</sup> cells were stained with LysoTracker Red and imaged by confocal microscopy (*top panels*). MEF-PS1/2<sup>-/-</sup> cells were treated with L803-mts (40  $\mu$ M), SB-216763 (5  $\mu$ M), and LiCl (20 mM) for 4 h. The cells were stained with LysoTracker Red and imaged by confocal microscopy (*bottom panels*). The scale bars represent 10  $\mu$ m. *C*, MEF-PS1/2<sup>-/-</sup> cells were treated with L803-mts (40  $\mu$ M), SB-216763 (5  $\mu$ M), and LiCl (20 mM). The lysosomes were partially purified as described under “Experimental Procedures.” Lysosome precipitates were immunoblotted for Lamp1, v-ATPase V0a1, CatD, and mCatD. The faint band corresponding to the 14-kDa mCatD is shown.

Our results are in line with accumulating evidence demonstrating the importance of the lysosomal system for A $\beta$  clearance and AD pathogenesis. Indeed, lysosome function declines with age (72), and CatD activity was previously shown to be correlated with neuroprotection from degenerative disease (63, 73). Inhibition of lysosomal activity increased brain A $\beta$  loads that were diminished by enhanced cathepsin activities (27, 74). In addition, the anti-amyloidogenic role of lysosomal proteolysis has been demonstrated in storage disease models (28), and enhanced lysosomal activity triggered by a pharmacological activator reduces A $\beta$  pathology and ameliorates behavioral deficits in different AD mouse models (26, 75). Given the role of lysosomes in amyloid clearance, it is tempting to suggest that deficits in lysosomal acidification observed in the 5XFAD brain contribute to the rapid and massive accumulation of A $\beta$  loads observed in these mice (31). Hence, restoration of lysosomal activity by L803-mts was probably responsible, at least in part, for the clearance in A $\beta$  deposits observed in the treated mice. It is important to note that L803-mts had a preventative effect, because treatment was begun prior the appearance of A $\beta$  pathology. Our results corroborate previous studies that showed that inhibition in GSK-3 activity reduced A $\beta$  production and/or A $\beta$  pathology (14, 16, 17). The one study that showed that knock-out of GSK-3 $\alpha$  or GSK-3 $\beta$  in the mouse brain did not affect APP metabolism or A $\beta$  levels (15) was performed using an *in vivo* model that lacked A $\beta$  pathology, and the role of GSK-3 might have been masked under these conditions.

An additional important finding of our study is the demonstration of GSK-3 as a “positive regulator” of the mTOR pathway. We previously reported that GSK-3 activated the mTOR target eEF-2 (29), and another study showed GSK-3 activation of mTOR in cancer cells (29, 30). Thus, reactivation of mTOR by L803-mts in the 5XFAD brain was not mediated by direct

inhibition of GSK-3. Rather, we suggest that disrupted lysosomal activity and elevated APP/A $\beta$  burdens are responsible for inhibition of mTOR in the 5XFAD brain and that normalization of lysosomal activity enabled normalization in mTOR activity. Furthermore, the reduction in A $\beta$  deposits upon GSK-3 inhibition is an additional factor that enables reactivation of mTOR. Previous studies indeed provide a support for a tight link between lysosomal regulation and mTOR (23, 24), and others have demonstrated inhibition of mTOR by A $\beta$  peptides (76, 77). It is noteworthy that aberrant regulation of mTOR has been implicated in behavior dysfunctions and memory loss (21, 22). Reduced mTOR activity was reported in AD patients (77) and was demonstrated in subjects with impaired synaptic plasticity and cognitive functions (76–78). On the other hand, activation of mTOR has been shown to improve cognitive deficits and was linked with reduction in A $\beta$  pathology (76, 77). Hence, reduced mTOR activity in the brains of 5XFAD mice could be well attributed to their cognitive decline, and restoration of mTOR activity by L803-mts repaired (in part) cognitive deficits. Altogether, we suggest that reacidification of lysosomes enhanced A $\beta$  burden clearance and enabled reactivation of mTOR, which, in turn, reversed AD pathogenesis (summarized in Fig. 8).

Although previous studies indicated a role for autophagy in  $\beta$ -amyloid clearance (56, 79), we did not find indications for enhanced autophagy in brains of L803-mts-treated mice. We observed a reduced LC3II/LC3I ratio and increased p62/SQSTM1, indicating that autophagy was suppressed in the L803-mts-treated mouse brain. Reactivation of mTOR, a primary autophagy suppressor (54, 60, 61), detected in brains of L803-mts-treated mice, was likely responsible for inhibited autophagy. Hence, lysosomal activity enhanced clearance of A $\beta$  loads independent of autophagy. Indeed, autophagy-indepen-

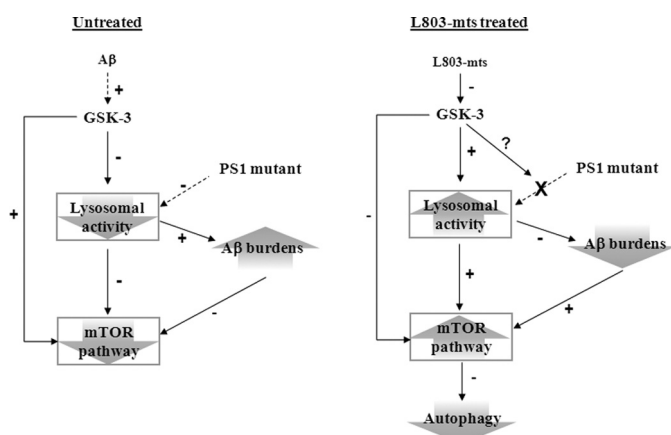


**FIGURE 8. Molecular mechanisms controlling GSK-3, lysosomes, mTOR, and A $\beta$  burdens in the 5XFAD brain.** In brains of untreated mice, GSK-3 is activated by A $\beta$  peptides. Hyperactive GSK-3 and mutant PS1 impair lysosomal acidification. This, in turn, accelerates accumulation of A $\beta$  burdens. GSK-3 activates mTOR, but mTOR is also inhibited by the disruption in lysosome activity and by accumulated APP/A $\beta$  burdens. The “net” effect on mTOR activity is inhibition. In L803-mts-treated mice, inhibition of GSK-3 restores lysosomal acidification and in addition prevents the deleterious effect of mutant PS1 on lysosomal acidification (by yet unknown mechanism). The normalization in lysosomal activity results in reduced A $\beta$  burdens. Lowering of A $\beta$  burdens and restoring lysosomal activity enable reactivation of mTOR, which inhibits autophagy. *Minus signs* mark inhibition, *plus signs* mark activation, and *dashed arrows* indicate processes reported in the literature.

dent, lysosomal-mediated APP processing and A $\beta$  clearance has been demonstrated previously (26, 28).

The GSK-3 isozymes did not appear to have different roles in regulation of mTOR or lysosomal acidification. This was not an unexpected observation because GSK-3 isozymes frequently show redundant activity (for example, as in Ref. 80). It should be noted, however, that GSK-3 $\alpha$  was previously implicated in A $\beta$  production (14) and A $\beta$  plaque formation (17). Thus, it is possible that GSK-3 isozymes influence A $\beta$  pathology by similar and by distinct pathways (14, 16, 81, 82).

Recent studies showed that PS1 is essential for lysosomal acidification (69, 71, 83) and implicated defects in glycosylation of v-ATPase subunit V0a1 as the cause of impaired lysosomal acidification in PS1-deficient cells (69). Treatment with L803-mts restored impaired lysosomal acidification in PS1/2-deficient cells, indicating that inhibition of GSK-3 could compensate for impaired lysosomal acidification caused by dysfunctional PS1. This suggested a possible cross-talk between presenilins and GSK-3 signaling that should be further investigated. Like deficits in PS1, hyperactive GSK-3 may contribute to impaired lysosomal acidification detected in the 5XFAD mice brains, and the mechanism that underlies this impairment may be shared.

In summary, we show that GSK-3 contributes to A $\beta$  pathology developed in the AD mouse brain. We suggest that by normalizing lysosomal acidification and reactivation of mTOR, the GSK-3 inhibitor, L803-mts, inhibits accumulation of A $\beta$  burdens and ameliorates cognitive function. GSK-3 thus appears to be a novel drug target for the treatment of AD.

## REFERENCES

1. Selkoe, D. J. (2001) Alzheimer's disease. Genes, proteins, and therapy. *Physiol. Rev.* **81**, 741–766
2. De Strooper, B. (2010) Proteases and proteolysis in Alzheimer disease. A

- multifactorial view on the disease process. *Physiol. Rev.* **90**, 465–494
3. Hardy, J. (2009) The amyloid hypothesis for Alzheimer's disease. A critical reappraisal. *J. Neurochem.* **110**, 1129–1134
4. Näslund, J., Haroutunian, V., Mohs, R., Davis, K. L., Davies, P., Greengard, P., and Buxbaum, J. D. (2000) Correlation between elevated levels of amyloid  $\beta$ -peptide in the brain and cognitive decline. *JAMA* **283**, 1571–1577
5. Karran, E., Mercken, M., and De Strooper, B. (2011) The amyloid cascade hypothesis for Alzheimer's disease. An appraisal for the development of therapeutics. *Nat. Rev. Drug Discov.* **10**, 698–712
6. Jonsson, T. (2012) A mutation in APP protects against Alzheimer's disease and age-related cognitive decline. *Nature* **488**, 96–99
7. Woodgett, J. R. (1990) Molecular cloning and expression of glycogen synthase kinase-3/factor A. *EMBO J.* **9**, 2431–2438
8. Gómez-Sintes, R., Hernández, F., Lucas, J. J., and Avila, J. (2011) GSK-3 mouse models to study neuronal apoptosis and neurodegeneration. *Front. Mol. Neurosci.* **4**, 45
9. Hooper, C., Killick, R., and Lovestone, S. (2008) The GSK3 hypothesis of Alzheimer's disease. *J. Neurochem.* **104**, 1433–1439
10. Terwel, D., Muyliaert, D., Dewachter, I., Borghgraef, P., Croes, S., Devijver, H., and Van Leuven, F. (2008) Amyloid activates GSK-3 $\beta$  to aggravate neuronal tauopathy in bigenic mice. *Am. J. Pathol.* **172**, 786–798
11. Jope, R. S., Yuskaitis, C. J., and Beurel, E. (2007) Glycogen synthase kinase-3 (GSK3). Inflammation, diseases, and therapeutics. *Neurochem. Res.* **32**, 577–595
12. Huang, H. C., and Klein, P. S. (2006) Multiple roles for glycogen synthase kinase-3 as a drug target in Alzheimer's disease. *Curr. Drug Targets* **7**, 1389–1397
13. Eldar-Finkelman, H., and Martinez, A. (2011) GSK-3 inhibitors. Preclinical and clinical focus on CNS. *Front. Mol. Neurosci.* **4**, 32
14. Phiel, C. J., Wilson, C. A., Lee, V. M., and Klein, P. S. (2003) GSK-3 $\alpha$  regulates production of Alzheimer's disease amyloid- $\beta$  peptides. *Nature* **423**, 435–439
15. Jaworski, T., Dewachter, I., Lechat, B., Gees, M., Kremer, A., Demedts, D., Borghgraef, P., Devijver, H., Kügler, S., Patel, S., Woodgett, J. R., and Van Leuven, F. (2011) GSK-3 $\alpha$ /b kinases and amyloid production *in vivo*. *Nature* **480**, E4–E5
16. Serenó, L., Coma, M., Rodríguez, M., Sánchez-Ferrer, P., Sánchez, M. B., Gich, I., Agulló, J. M., Pérez, M., Avila, J., Guardia-Laguarta, C., Clarimón, J., Lleó, A., and Gómez-Isla, T. (2009) A novel GSK-3 $\beta$  inhibitor reduces Alzheimer's pathology and rescues neuronal loss *in vivo*. *Neurobiol. Dis.* **35**, 359–367
17. Hurtado, D. E., Molina-Porcel, L., Carroll, J. C., Macdonald, C., Aboagye, A. K., Trojanowski, J. Q., and Lee, V. M. (2012) Selectively silencing GSK-3 isoforms reduces plaques and tangles in mouse models of Alzheimer's disease. *J. Neurosci.* **32**, 7392–7402
18. Laplante, M., and Sabatini, D. M. (2012) mTOR signaling in growth control and disease. *Cell* **149**, 274–293
19. Hay, N., and Sonenberg, N. (2004) Upstream and downstream of mTOR. *Genes Dev.* **18**, 1926–1945
20. Wullschlegel, S., Loewith, R., and Hall, M. N. (2006) TOR signaling in growth and metabolism. *Cell* **124**, 471–484
21. Costa-Mattoli, M., Sossin, W. S., Klann, E., and Sonenberg, N. (2009) Translational control of long-lasting synaptic plasticity and memory. *Neuron* **61**, 10–26
22. Swiech, L., Perycz, M., Malik, A., and Jaworski, J. (2008) Role of mTOR in physiology and pathology of the nervous system. *Biochim. Biophys. Acta* **1784**, 116–132
23. Zoncu, R., Bar-Peled, L., Efeyan, A., Wang, S., Sancak, Y., and Sabatini, D. M. (2011) mTORC1 senses lysosomal amino acids through an inside-out mechanism that requires the vacuolar H<sup>+</sup>-ATPase. *Science* **334**, 678–683
24. Korolchuk, V. I., Saiki, S., Lichtenberg, M., Siddiqi, F. H., Roberts, E. A., Imarisio, S., Jahress, L., Sarkar, S., Futter, M., Menzies, F. M., O'Kane, C. J., Deretic, V., and Rubinsztein, D. C. (2011) Lysosomal positioning coordinates cellular nutrient responses. *Nat. Cell Biol.* **13**, 453–460
25. Vila, M., Bové, J., Dehay, B., Rodríguez-Muela, N., and Boya, P. (2011) Lysosomal membrane permeabilization in Parkinson disease. *Autophagy* **7**, 98–100

26. Butler, D., Hwang, J., Estick, C., Nishiyama, A., Kumar, S. S., Baveghems, C., Young-Oxendine, H. B., Wisniewski, M. L., Charalambides, A., and Bahr, B. A. (2011) Protective effects of positive lysosomal modulation in Alzheimer's disease transgenic mouse models. *PLoS One* **6**, e20501
27. Yang, D. S., Stavrides, P., Mohan, P. S., Kaushik, S., Kumar, A., Ohno, M., Schmidt, S. D., Wesson, D., Bandyopadhyay, U., Jiang, Y., Pawlik, M., Peterhoff, C. M., Yang, A. J., Wilson, D. A., St George-Hyslop, P., Westaway, D., Mathews, P. M., Levy, E., Cuervo, A. M., and Nixon, R. A. (2011) Reversal of autophagy dysfunction in the TgCRND8 mouse model of Alzheimer's disease ameliorates amyloid pathologies and memory deficits. *Brain* **134**, 258–277
28. Boland, B., Smith, D. A., Mooney, D., Jung, S. S., Walsh, D. M., and Platt, F. M. (2010) Macroautophagy is not directly involved in the metabolism of amyloid precursor protein. *J. Biol. Chem.* **285**, 37415–37426
29. Karyo, R., Eskira, Y., Pinhasov, A., Belmaker, R., Agam, G., and Eldar-Finkelman, H. (2010) Identification of eukaryotic elongation factor-2 as a novel cellular target of lithium and glycogen synthase kinase-3. *Mol. Cell Neurosci.* **45**, 449–455
30. Shin, S., Wolgamott, L., Yu, Y., Blenis, J., and Yoon, S. O. (2011) Glycogen synthase kinase (GSK)-3 promotes p70 ribosomal protein S6 kinase (p70S6K) activity and cell proliferation. *Proc. Natl. Acad. Sci. U.S.A.* **108**, E1204–1213
31. Oakley, H., Cole, S. L., Logan, S., Maus, E., Shao, P., Craft, J., Guillozet-Bongaarts, A., Ohno, M., Disterhoft, J., Van Eldik, L., Berry, R., and Vassar, R. (2006) Intraneuronal  $\beta$ -amyloid aggregates, neurodegeneration, and neuron loss in transgenic mice with five familial Alzheimer's disease mutations. Potential factors in amyloid plaque formation. *J. Neurosci.* **26**, 10129–10140
32. Plotkin, B., Kaidanovich, O., Talior, I., and Eldar-Finkelman, H. (2003) Insulin mimetic action of synthetic phosphorylated peptide inhibitors of glycogen synthase kinase-3. *J. Pharmacol. Exp. Ther.* **305**, 974–980
33. Kaidanovich-Beilin, O., and Eldar-Finkelman, H. (2006) Long-term treatment with novel glycogen synthase kinase-3 inhibitor improves glucose homeostasis in ob/ob mice. Molecular characterization in liver and muscle. *J. Pharmacol. Exp. Ther.* **316**, 17–24
34. Rao, R., Hao, C. M., Redha, R., Wasserman, D. H., McGuinness, O. P., and Breyer, M. D. (2007) Glycogen synthase kinase 3 inhibition improves insulin-stimulated glucose metabolism but not hypertension in high-fat-fed C57BL/6J mice. *Diabetologia* **50**, 452–460
35. Chen, G., Bower, K. A., Ma, C., Fang, S., Thiele, C. J., and Luo, J. (2004) Glycogen synthase kinase 3 $\beta$  (GSK3 $\beta$ ) mediates 6-hydroxydopamine-induced neuronal death. *FASEB J.* **18**, 1162–1164
36. Kaidanovich-Beilin, O., Milman, A., Weizman, A., Pick, C. G., and Eldar-Finkelman, H. (2004) Rapid anti-depressive like activity of specific GSK-3 inhibitor, and its effect on  $\beta$ -catenin in the mouse hippocampus. *Biol. Psychiatry* **55**, 781–784
37. Kim, W. Y., Zhou, F. Q., Zhou, J., Yokota, Y., Wang, Y. M., Yoshimura, T., Kaibuchi, K., Woodgett, J. R., Anton, E. S., and Snider, W. D. (2006) Essential roles for GSK-3s and GSK-3-primed substrates in neurotrophin-induced and hippocampal axon growth. *Neuron* **52**, 981–996
38. Saura, C. A., Chen, G., Malkani, S., Choi, S. Y., Takahashi, R. H., Zhang, D., Gouras, G. K., Kirkwood, A., Morris, R. G., and Shen, J. (2005) Conditional inactivation of presenilin 1 prevents amyloid accumulation and temporarily rescues contextual and spatial working memory impairments in amyloid precursor protein transgenic mice. *J. Neurosci.* **25**, 6755–6764
39. Herreman, A., Van Gassen, G., Bentahir, M., Nyabi, O., Craessaerts, K., Mueller, U., Annaert, W., and De Strooper, B. (2003)  $\gamma$ -Secretase activity requires the presenilin-dependent trafficking of nicastrin through the Golgi apparatus but not its complex glycosylation. *J. Cell Sci.* **116**, 1127–1136
40. Born, J., Lange, T., Kern, W., McGregor, G. P., Bickel, U., and Fehm, H. L. (2002) Sniffing neuropeptides. A transnasal approach to the human brain. *Nat. Neurosci.* **5**, 514–516
41. Illum, L. (2000) Transport of drugs from the nasal cavity to the central nervous system. *Eur. J. Pharm. Sci.* **11**, 1–18
42. Rubinfeld, B., Albert, I., Porfiri, E., Fiol, C., Munemitsu, S., and Polakis, P. (1996) Binding of GSK-3 $\beta$  to the APC- $\beta$ -catenin complex and regulation of complex assembly. *Science* **272**, 1023–1026
43. Ikeda, S., Kishida, S., Yamamoto, H., Murai, H., Koyama, S., and Kikuchi, A. (1998) Axin, a negative regulator of the Wnt signaling pathway, forms a complex with GSK-3 $\beta$  and  $\beta$ -catenin and promotes GSK-3 $\beta$ -dependent phosphorylation of  $\beta$ -catenin. *EMBO J.* **17**, 1371–1384
44. Zhang, Z., Hartmann, H., Do, V. M., Abramowski, D., Sturchler-Pierrat, C., Staufenbiel, M., Sommer, B., van de Wetering, M., Clevers, H., Saftig, P., De Strooper, B., He, X., and Yankner, B. A. (1998) Destabilization of  $\beta$ -catenin by mutations in presenilin-1 potentiates neuronal apoptosis. *Nature* **395**, 698–702
45. Frydman-Marom, A., Levin, A., Farfara, D., Benromano, T., Scherzer-Attali, R., Peled, S., Vassar, R., Segal, D., Gazit, E., Frenkel, D., and Ovadia, M. (2011) Orally administered cinnamon extract reduces  $\beta$ -amyloid oligomerization and corrects cognitive impairment in Alzheimer's disease animal models. *PLoS One* **6**, e16564
46. Eckman, E. A., and Eckman, C. B. (2005) A $\beta$ -degrading enzymes. Modulators of Alzheimer's disease pathogenesis and targets for therapeutic intervention. *Biochem. Soc. Trans.* **33**, 1101–1105
47. Benedict, C., Hallschmid, M., Hatke, A., Schultes, B., Fehm, H. L., Born, J., and Kern, W. (2004) Intranasal insulin improves memory in humans. *Psychoneuroendocrinology* **29**, 1326–1334
48. Gasparini, L., Netzer, W. J., Greengard, P., and Xu, H. (2002) Does insulin dysfunction play a role in Alzheimer's disease? *Trends Pharmacol. Sci.* **23**, 288–293
49. Yamamoto, A., Cremona, M. L., and Rothman, J. E. (2006) Autophagy-mediated clearance of huntingtin aggregates triggered by the insulin-signaling pathway. *J. Cell Biol.* **172**, 719–731
50. Song, B., Lai, B., Zheng, Z., Zhang, Y., Luo, J., Wang, C., Chen, Y., Woodgett, J. R., and Li, M. (2010) Inhibitory phosphorylation of GSK-3 by CaMKII couples depolarization to neuronal survival. *J. Biol. Chem.* **285**, 41122–41134
51. Fang, X., Yu, S. X., Lu, Y., Bast, R. C., Jr., Woodgett, J. R., and Mills, G. B. (2000) Phosphorylation and inactivation of glycogen synthase kinase 3 by protein kinase A. *Proc. Natl. Acad. Sci. U.S.A.* **97**, 11960–11965
52. Eldar-Finkelman, H., Seger, R., Vandenheede, J. R., and Krebs, E. G. (1995) Inactivation of glycogen synthase kinase-3 by epidermal growth factor is mediated by mitogen-activated protein kinase/p90 ribosomal protein S6 kinase signaling pathway in NIH/3T3 cells. *J. Biol. Chem.* **270**, 987–990
53. Hernández, F., Langa, E., Cuadros, R., Avila, J., and Villanueva, N. (2010) Regulation of GSK3 isoforms by phosphatases PP1 and PP2A. *Mol. Cell Biochem.* **344**, 211–215
54. Klionsky, D. J. (2007) Autophagy. From phenomenology to molecular understanding in less than a decade. *Nat. Rev. Mol. Cell Biol.* **8**, 931–937
55. Levine, B., and Kroemer, G. (2008) Autophagy in the pathogenesis of disease. *Cell* **132**, 27–42
56. Yu, W. H., Cuervo, A. M., Kumar, A., Peterhoff, C. M., Schmidt, S. D., Lee, J. H., Mohan, P. S., Mercken, M., Farmery, M. R., Tjernberg, L. O., Jiang, Y., Duff, K., Uchiyama, Y., Näslund, J., Mathews, P. M., Cataldo, A. M., and Nixon, R. A. (2005) Macroautophagy. A novel  $\beta$ -amyloid peptide-generating pathway activated in Alzheimer's disease. *J. Cell Biol.* **171**, 87–98
57. Mizushima, N., and Yoshimori, T. (2007) How to interpret LC3 immunoblotting. *Autophagy* **3**, 542–545
58. Kabeya, Y., Mizushima, N., Ueno, T., Yamamoto, A., Kirisako, T., Noda, T., Kominami, E., Ohsumi, Y., and Yoshimori, T. (2000) LC3, a mammalian homologue of yeast Apg8p, is localized in autophagosome membranes after processing. *EMBO J.* **19**, 5720–5728
59. Bjørkøy, G., Lamark, T., Brech, A., Outzen, H., Perander, M., Overvatn, A., Stenmark, H., and Johansen, T. (2005) p62/SQSTM1 forms protein aggregates degraded by autophagy and has a protective effect on huntingtin-induced cell death. *J. Cell Biol.* **171**, 603–614
60. Rubinsztein, D. C., Gestwicki, J. E., Murphy, L. O., and Klionsky, D. J. (2007) Potential therapeutic applications of autophagy. *Nat. Rev. Drug Discov.* **6**, 304–312
61. Yu, L., McPhee, C. K., Zheng, L., Mardones, G. A., Rong, Y., Peng, J., Mi, N., Zhao, Y., Liu, Z., Wan, F., Hailey, D. W., Oorschot, V., Klumperman, J., Baehrecke, E. H., and Lenardo, M. J. (2010) Termination of autophagy and reformation of lysosomes regulated by mTOR. *Nature* **465**, 942–946
62. Proud, C. G. (2004) mTOR-mediated regulation of translation factors by amino acids. *Biochem. Biophys. Res. Commun.* **313**, 429–436

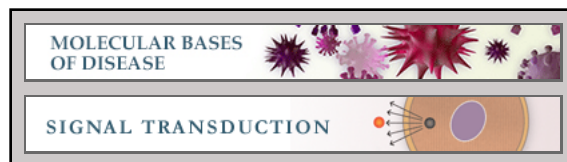
63. Qiao, L., Hamamichi, S., Caldwell, K. A., Caldwell, G. A., Yacoubian, T. A., Wilson, S., Xie, Z. L., Speake, L. D., Parks, R., Crabtree, D., Liang, Q., Crimmins, S., Schneider, L., Uchiyama, Y., Iwatsubo, T., Zhou, Y., Peng, L., Lu, Y., Standaert, D. G., Walls, K. C., Shacka, J. J., Roth, K. A., and Zhang, J. (2008) Lysosomal enzyme cathepsin D protects against  $\alpha$ -synuclein aggregation and toxicity. *Mol. Brain* **1**, 17
64. Saftig, P., and Klumperman, J. (2009) Lysosome biogenesis and lysosomal membrane proteins. Trafficking meets function. *Nat. Rev. Mol. Cell Biol.* **10**, 623–635
65. Luzio, J. P., Pryor, P. R., and Bright, N. A. (2007) Lysosomes. Fusion and function. *Nat. Rev. Mol. Cell Biol.* **8**, 622–632
66. Hinton, A., Sennoune, S. R., Bond, S., Fang, M., Reuveni, M., Sahagian, G. G., Jay, D., Martinez-Zaguilan, R., and Forgac, M. (2009) Function of a subunit isoforms of the V-ATPase in pH homeostasis and in vitro invasion of MDA-MB231 human breast cancer cells. *J. Biol. Chem.* **284**, 16400–16408
67. Mindell, J. A. (2012) Lysosomal acidification mechanisms. *Annu. Rev. Physiol.* **74**, 69–86
68. Gieselmann, V., Hasilik, A., and von Figura, K. (1985) Processing of human cathepsin D in lysosomes in vitro. *J. Biol. Chem.* **260**, 3215–3220
69. Lee, J. H., Yu, W. H., Kumar, A., Lee, S., Mohan, P. S., Peterhoff, C. M., Wolfe, D. M., Martinez-Vicente, M., Massey, A. C., Sovak, G., Uchiyama, Y., Westaway, D., Cuervo, A. M., and Nixon, R. A. (2010) Lysosomal proteolysis and autophagy require presenilin 1 and are disrupted by Alzheimer-related PS1 mutations. *Cell* **141**, 1146–1158
70. Williamson, W. R., and Hiesinger, P. R. (2010) On the role of v-ATPase V0a1-dependent degradation in Alzheimer disease. *Commun. Integr. Biol.* **3**, 604–607
71. Neely, K. M., Green, K. N., and LaFerla, F. M. (2011) Presenilin is necessary for efficient proteolysis through the autophagy-lysosome system in a  $\gamma$ -secretase-independent manner. *J. Neurosci.* **31**, 2781–2791
72. Cuervo, A. M., and Dice, J. F. (2000) When lysosomes get old. *Exp. Gerontol.* **35**, 119–131
73. Steinfeld, R., Reinhardt, K., Schreiber, K., Hillebrand, M., Kraetzner, R., Bruck, W., Saftig, P., and Gartner, J. (2006) Cathepsin D deficiency is associated with a human neurodegenerative disorder. *Am. J. Hum. Genet.* **78**, 988–998
74. Yang, D. S., Stavrides, P., Mohan, P. S., Kaushik, S., Kumar, A., Ohno, M., Schmidt, S. D., Wesson, D. W., Bandyopadhyay, U., Jiang, Y., Pawlik, M., Peterhoff, C. M., Yang, A. J., Wilson, D. A., St George-Hyslop, P., Westaway, D., Mathews, P. M., Levy, E., Cuervo, A. M., and Nixon, R. A. (2011) Therapeutic effects of remediating autophagy failure in a mouse model of Alzheimer disease by enhancing lysosomal proteolysis. *Autophagy* **7**, 788–789
75. Sun, B., Zhou, Y., Halabisky, B., Lo, I., Cho, S. H., Mueller-Steiner, S., Devidze, N., Wang, X., Grubb, A., and Gan, L. (2008) Cystatin C-cathepsin B axis regulates amyloid  $\beta$  levels and associated neuronal deficits in an animal model of Alzheimer's disease. *Neuron* **60**, 247–257
76. Ma, T., Hoefler, C. A., Capetillo-Zarate, E., Yu, F., Wong, H., Lin, M. T., Tampellini, D., Klann, E., Blitzer, R. D., and Gouras, G. K. (2010) Dysregulation of the mTOR pathway mediates impairment of synaptic plasticity in a mouse model of Alzheimer's disease. *PLoS One* **5**, e12845
77. Lafay-Chebassier, C., Paccalin, M., Page, G., Barc-Pain, S., Perault-Pochat, M. C., Gil, R., Pradier, L., and Hugon, J. (2005) mTOR/p70S6k signalling alteration by A $\beta$  exposure as well as in APP-PS1 transgenic models and in patients with Alzheimer's disease. *J. Neurochem.* **94**, 215–225
78. Stoica, L., Zhu, P. J., Huang, W., Zhou, H., Kozma, S. C., and Costa-Mattioli, M. (2011) Selective pharmacogenetic inhibition of mammalian target of rapamycin complex I (mTORC1) blocks long-term synaptic plasticity and memory storage. *Proc. Natl. Acad. Sci. U.S.A.* **108**, 3791–3796
79. Pickford, F., Masliah, E., Britschgi, M., Lucin, K., Narasimhan, R., Jaeger, P. A., Small, S., Spencer, B., Rockenstein, E., Levine, B., and Wyss-Coray, T. (2008) The autophagy-related protein beclin 1 shows reduced expression in early Alzheimer disease and regulates amyloid  $\beta$  accumulation in mice. *J. Clin. Invest.* **118**, 2190–2199
80. Doble, B. W., Patel, S., Wood, G. A., Kockeritz, L. K., and Woodgett, J. R. (2007) Functional redundancy of GSK-3 $\alpha$  and GSK-3 $\beta$  in Wnt/ $\beta$ -catenin signaling shown by using an allelic series of embryonic stem cell lines. *Dev. Cell* **12**, 957–971
81. Sun, X., Sato, S., Murayama, O., Murayama, M., Park, J. M., Yamaguchi, H., and Takashima, A. (2002) Lithium inhibits amyloid secretion in COS7 cells transfected with amyloid precursor protein C100. *Neurosci. Lett.* **321**, 61–64
82. Li, B., Ryder, J., Su, Y., Zhou, Y., Liu, F., and Ni, B. (2003) FRAT1 peptide decreases A $\beta$  production in swAPP<sub>751</sub> cells. *FEBS Lett.* **553**, 347–350
83. Cataldo, A. M., Peterhoff, C. M., Schmidt, S. D., Terio, N. B., Duff, K., Beard, M., Mathews, P. M., and Nixon, R. A. (2004) Presenilin mutations in familial Alzheimer disease and transgenic mouse models accelerate neuronal lysosomal pathology. *J. Neuropathol. Exp. Neurol.* **63**, 821–830

**Molecular Bases of Disease:**  
**Inhibition of Glycogen Synthase Kinase-3  
Ameliorates  $\beta$ -Amyloid Pathology and  
Restores Lysosomal Acidification and  
Mammalian Target of Rapamycin Activity  
in the Alzheimer Disease Mouse Model: IN  
VIVO AND IN VITRO STUDIES**

Limor Avrahami, Dorit Farfara, Maya  
Shaham-Kol, Robert Vassar, Dan Frenkel and  
Hagit Eldar-Finkelman

*J. Biol. Chem.* 2013, 288:1295-1306.

doi: 10.1074/jbc.M112.409250 originally published online November 15, 2012



Access the most updated version of this article at doi: [10.1074/jbc.M112.409250](https://doi.org/10.1074/jbc.M112.409250)

Find articles, minireviews, Reflections and Classics on similar topics on the [JBC Affinity Sites](#).

Alerts:

- [When this article is cited](#)
- [When a correction for this article is posted](#)

[Click here](#) to choose from all of JBC's e-mail alerts

This article cites 83 references, 27 of which can be accessed free at  
<http://www.jbc.org/content/288/2/1295.full.html#ref-list-1>